**Research article**

# Primary restriction of S-RNase cytotoxicity by a stepwise ubiquitination and degradation pathway in *Petunia hybrida*

Hong Zhao[1,2 †], Yanzhai Song[1,2 †], Junhui Li[1,2], Yue Zhang[1,2], Huaqiu Huang[1,2], Qun Li[1], Yu'e Zhang[1], Yongbiao Xue[1,2,3,4 *]

[1]State Key Laboratory of Plant Cell and Chromosome Engineering, Institute of Genetics and Developmental Biology, and The Innovation Academy of Seed Design, Chinese Academy of Sciences, Beijing 100101, China

[2]University of Chinese Academy of Sciences, Beijing 100049, China

[3]Beijing Institute of Genomics, Chinese Academy of Sciences, and National Centre for Bioinformation, Beijing 100101, China

[4]Jiangsu Co-Innovation Center for Modern Production Technology of Grain Crops, Yangzhou University, Yangzhou 225009, China



This article has been accepted for publication and undergone full peer review but has not been through the copyediting, typesetting, pagination and proofreading process, which may lead to differences between this version and the Version of Record. Please cite this article as doi: 10.1111/NPH.17438

†**Contributed equally to this work**

*__Author for correspondence__

**E-mail:** ybxue@genetics.ac.cn

**Phone:** +86-01-6480-1181

**ORCID:** 0000-0002-6895-8472

Received: 24 December 2020

Accepted: 20 April 2021

**Summary**

- In self-incompatible *Petunia* species, the pistil S-RNase acts as cytotoxin to inhibit self-pollination but is polyubiquitinated by the pollen-specific non-self *S*-locus F-box (SLF) proteins and subsequently degraded by the ubiquitin-proteasome system (UPS), allowing cross-pollination. However, it remains unclear how S-RNase is restricted by the UPS.
- Using biochemical analyses, we first show that *Petunia hybrida* $S_3$-RNase is largely ubiquitinated by K48-linked polyubiquitin chains at three regions, R I, II and III. R I is ubiquitinated in unpollinated, self- and cross-pollinated pistils, indicating its occurrence before $PhS_3$-RNase uptake into pollen tubes, whereas R II and III are exclusively ubiquitinated in cross-pollinated pistils.
- Transgenic analyses showed that removal of R II ubiquitination resulted in significantly reduced seed sets from cross-pollination and that of R I and III in less extent, indicating their increased cytotoxicity. Consistent with this, the mutated R II of $PhS_3$-RNase resulted in a marked reduction of its degradation, whereas that of R I and III in less reduction.
- Taken together, we demonstrate that $PhS_3$-RNase R II functions as a major ubiquitination region for its destruction and R I and III as minor ones, revealing that its cytotoxicity is primarily restricted by a stepwise UPS mechanism for cross-pollination in *P. hybrida*.

**Keywords:** ubiquitination, self-incompatibility, S-RNase, SLF, *Petunia hybrida*

## Introduction

Self-incompatibility (SI), an inability of a fertile seed plant to produce zygote after self-pollination, represents a reproductive barrier adopted by nearly 40% of flowering plant species to prevent self-fertilization and to promote outcrossing (De Nettancourt, 2001). In many species, SI is usually controlled by a single multi-allelic *S*-locus encoding both male and female *S* determinants (De Nettancourt, 2001; Takayama and Isogai, 2005; Franklin-Tong, 2008; Zhang et al., 2009). Their molecular interaction confers the pistil an ability to distinguish between genetically related self- and non-self-pollen. In general, SI can be classified into self- and non-self-recognition systems based on their distinct molecular mechanisms (Fujii et al., 2016). In the self-recognition system of Papaveraceae and Brassicaceae, self-pollen rejection occurs as a specific interaction between the *S* determinants from the same *S* haplotype. In *Papaver rhoeas*, the female *S*-determinant Prs S (*P. rhoeas* stigmatic S) interacts with its cognate Prp S (*P. rhoeas* pollen S) to stimulate a signaling cascade leading to programmed cell death (PCD) of self-pollen (Foote et al., 1994; Thomas and Franklin-Tong, 2004; Wheeler et al., 2009; Wilkins et al., 2014). In Brassicaceae, SI response is initiated by the specific interaction of the stigma *S*-locus receptor kinase (SRK) and its cognate pollen-coat-localized ligand *S*-locus cysteine-rich protein (SCR/SP11), triggering a phosphorylation-mediated signaling pathway resulting in the destruction of factors indispensable for pollen compatibility by the UPS (Schopfer et al., 1999; Suzuki et al., 1999; Takasaki et al., 2000; Takayama et al., 2000; Kakita et al., 2007; Samuel et al., 2008; Samuel et al., 2009; Ma et al., 2016). S-RNase-based SI, also termed as Solanaceae-type SI, is a well-studied non-self-recognition system widely present in Solanaceae, Plantaginaceae, Rosaceae and Rutaceae (Anderson et al., 1986; McClure et al., 1989; Sassa et al., 1996; Xue et al., 1996; Lai et al., 2002; Ushijima et al., 2003; Sijacic et al., 2004; Liang et al., 2020). In self-incompatible *Antirrhinum* and *Petunia* species, the pistil *S* determinant S-RNase serving as cytotoxin can be recognized and ubiquitinated by multiple pollen *S* determinants SLFs forming functional SCF ubiquitin ligases in a collaborative non-self-recognition manner, thus restricting cytotoxicity of non-self S-RNases resulting in cross-pollination (Qiao et al., 2004b; Hua and Kao, 2006; Hua et al., 2008; Hua and Kao, 2008; Zhang et al., 2009; Kubo et al., 2010; Liu et al., 2014).

However, it remains largely unclear how S-RNases are specifically regulated in the non-self-recognition system. Currently, two models, the S-RNase degradation model and the S-RNase compartmentalization model, have been proposed to explain how S-RNase cytotoxicity is restricted for cross-pollination (Qiao et al., 2004b; Goldraij et al., 2006; McClure, 2009; McClure et al., 2011; Liu et al., 2014). In the degradation model proposed in *Petunia hybrida*, both self and non-self S-RNases taken up by pollen tubes are mainly localized in the cytosol, where further recognized by SLFs. Entani et al. (2014) showed that $SCF^{SLF}$ complexes can specifically polyubiquitinate non-self S-RNases rather than self ones *in vitro* in *P. hybrida*, providing evidence for S-RNase ubiquitination by cross pollen. Whereas in self-pollen tubes, binding of self S-RNase and SLF leads to the formation of nonfunctional $SCF^{SLF}$ complex, thus resulting in the survival of self S-RNase to inhibit pollen tube growth. Together with the discoveries of $SCF^{SLF}$ complex components such as SLF-interacting SKP1-like 1 (SSK1) and Cullin1 in the species from Solanaceae, Plantaginaceae and Rosaceae (Huang et al., 2006; Zhao et al., 2010; Xu et al., 2013; Entani et al., 2014; Li and Chetelat, 2014), the degradation model appears to function in several species of flowering plants possessing S-RNase-based SI. In *Nicotiana* species, Goldraij et al. (2006) proposed that the majority of self- and non-self S-RNases would be sequestered in vacuole-like structures once imported into pollen tubes. Subsequently, self-recognition between SLFs and a small fraction of S-RNases localized in the cytosol would break the structures, releasing S-RNases in a late-stage of self-pollination, thus triggering the SI response. In contrast, non-self recognition could stabilize S-RNases and maintain their sequestration. Most previous studies showed that S-RNase degradation rather than compartmentalization acts as the major strategy to restrict S-RNase cytotoxicity in *P. hybrida* (Liu et al., 2014). Nevertheless, little is known about the linkage type of the polyubiquitin chains and the specific residue of S-RNase ubiquitinated by non-self $SCF^{SLF}$ complexes in cross-pollen tubes.

To address these questions, in this study, we first established an *in vivo* assay for examining polyubiquitination of $PhS_3$-RNase in cross-pollinated pistils and, together with *in vitro* ubiquitination analyses, we found that it is mainly ubiquitinated by K48-linked polyubiquitin chains in three regions named R I, II and III. Among them, R I ubiquitination occurs before

$PhS_3$-RNase entry into pollen tubes and likely mediated by an unknown E3 ligase, whereas R II and III are specifically ubiquitinated by $SCF^{SLF}$. Second, the ubiquitination removal of those three regions had little effect on the physicochemical properties of $PhS_3$-RNase, but negatively impacted their functions in cross-pollen tubes. The transgene with a mutated R II led to a significant reduction of seed sets from cross-pollination, whereas the mutated R I and III to much less extent in *P. hybrida*, showing that R II ubiquitination of $PhS_3$-RNase plays a major role in its destruction and cytotoxicity restriction, whereas R I and III minor roles. Furthermore, the ubiquitination removal of all three regions did not completely inhibit $PhS_3$-RNase degradation and cross seed sets, suggesting that the UPS is not the exclusive mechanism to restrict S-RNase cytotoxicity. Taken together, our results demonstrate a stepwise UPS mechanism for primary restriction of S-RNase cytotoxicity during cross-pollination in *P. hybrida*, providing novel mechanistic insight into a dynamic regulation of S-RNases.

## Materials and Methods

### Plant materials

Self-incompatible wild-type lines of $PhS_3S_3$, $PhS_VS_V$ and $PhS_3S_{3L}$ have been previously described (Robbins et al., 2000; Sims and Ordanic, 2001). The transgenic plants $PhS_3S_{3L}$/$PhS_{3L}$*SLF1-FLAG* were constructed by transforming $PhS_3S_{3L}$ with *pBI101-*$PhS_3$*A-SLF::*$PhS_{3L}$*SLF1-FLAG*. $PhS_3$*A-SLF* is a native promotor used for *PhSLFs* expression as previously described (Qiao et al., 2004a; Liu et al., 2014).

### Ti plasmid construction and transgenic plant generation

$PhS_3$*-RNase* cDNA and its *FLAG*-tagged form were amplified by primers listed in Table S1 to introduce *Xho*I and *Sac*I restriction sites at their 5' and 3' ends, respectively. $PhS_3$*-RNase* point mutations were generated by PCR (Polymerase chain reaction) using site-directed mutagenesis primers listed in Table S1. Ti plasmid constructs were separately electroporated into *Agrobacterium tumefaciens* strain LBA4404 and introduced into $PhS_3S_{3L}$ using the leaf disk

transformation method as described previously (Lee et al., 1994; Qiao et al., 2004a).

**Protein structure prediction and electrostatic potential analysis**

$PhS_3$-RNase protein structure was modeled by the I-TASSER server (http://zhanglab.ccmb.med.umich.edu/I-TASSER/) according to its instructions (Yang et al., 2015; Li et al., 2017). The first model generated by iterative simulations was selected for further analysis based on model quality evaluation using the VADAR version1.8 program (http://vadar.wishartlab.com) (Willard et al., 2003) and the ProSa-web program (https://prosa.services.came.sbg.ac.at/prosa.php) (Wiederstein and Sippl, 2007). Structures of point-mutated S-RNases were generated by mutagenesis in PyMol, and electrostatic potential analyses of $PhS_3$-RNase and its point-mutated structures were performed using plug-in APBS tools as previously described (Baker et al., 2001; Li et al., 2017).

**Quantitative (q) RT-PCR analysis**

Total RNAs were separately isolated from pistils derived from *$PhS_3S_{3L}$*/*$PhS_3$-RNase*- or *$PhS_3$-RNase* (*Mutant*) (*M*)-(*FLAG*) using TRIzol reagent (Ambion) according to the manufacturer's instructions. cDNA was subsequently synthesized using cDNA synthesis supermix (Transgen, AU311-02). qRT-PCR reaction mixes were prepared according to manufacturer's guidelines of ChamQ™ Universal SYBR qPCR Master Mix (Vazyme, Q711-02/03). Relevant primer sequences are listed in Table S1. qRT-PCR assays were performed by CFX96™ Real-Time System (Bio-Rad). *P. hybrida 18S rRNA* gene transcripts were used as an internal control. The data were analyzed with the method of Livak ($2^{-\Delta\Delta Ct}$) (Livak and Schmittgen, 2001).

**Mass spectrometry analysis for ubiquitination sites**

*$PhS_3S_{3L}$* plants were self- or cross-pollinated with *$PhS_3S_{3L}$*/*$PhS_{3L}$SLF1*. Then the pollinated pistils collected after 2, 6, 12 and 24 h, respectively, were mixed up, minced and lysed in buffer containing 7 M urea, 2 M thiourea and 0.1% CHAPS, and followed by 5-minute ultrasonication on ice. Samples of unpollinated pistils were prepared as controls. The lysate was centrifuged at 14,000 g for 10 min at 4°C and the supernatant was reduced with 10 mM DTT for 1 h at 56°C, and

subsequently alkylated with sufficient iodoacetamide for 1 h at room temperature in the dark (Udeshi et al., 2013b). Then the supernatant containing 10 mg protein was digested with Trypsin Gold (Promega) at enzyme-to-substrate 1:50 at 37°C for 16 h. Peptides were desalted with C18 cartridge and dried by vacuum centrifugation (Udeshi et al., 2013b), and then resuspended with MOPS IAP buffer (50 mM MOPS, 10 mM $KH_2PO_4$, 50 mM NaCl, pH 7.0) and centrifuged for 5 min at 12,000 g. The supernatants were incubated with anti-Ubiquitin Remnant Motif (K-ε-GG) beads (CST #5562, Cell Signaling Technology) for 2.5 h at 4°C and centrifuged for 30 s at 3,000 g at 4°C. Beads were washed in MOPS IAP buffer, then in water, prior to elution of the peptides with 0.15% TFA (Udeshi et al., 2013a). Then desalted by peptide desalting spin columns (Thermo Fisher, 89852) before LC-MS/MS analysis using Orbitrap Fusion mass spectrometer (Thermo Fisher). The resulting spectra from each fraction were searched separately against $PhS_3$-RNase amino acid sequences by the Maxquant search engines. Precursor quantification based on intensity was used for label-free quantification.

**S-RNase activity assay**

The coding sequences of *$PhS_3$-RNase* (without signal peptide) and *$PhS_3$-RNase* (*M*) were separately cloned into *pCold-TF* vector (Takara). Relevant primer sequences used are listed in Table S1. Trigger Factor (TF) is a 48 kDa soluble tag located at the N-terminus of His. The His-fused proteins were expressed in *Escherichia coli* Trans BL21 (DE3) plysS (Transgen) at 16℃ for 24 h at 180 rpm and purified using Ni Sepharose 6 Fast Flow beads (GE Healthcare, 10249123) according to the manufacturer's instructions. Protein concentration was determined by Bradford protein assays. The relative fluorescence units (RFU) of the recombinant proteins were monitored according to the manufacturer's instructions of RNase Alert Lab Test Kit (Ambion) using Synergy 2 (Biotech).

**Ubiquitination assay and immunoblotting**

The $SCF^{SLF\text{-}FLAG}$ complex attached to anti-FLAG M2 affinity gel (Sigma-Aldrich) was purified from *$PhS_3S_{3L}$*/*$PhS_{3L}$SLF1-FLAG* pollen tubes as described (Li et al., 2017), with that from *$PhS_3S_{3L}$* as a negative control. $PhS_3$-RNase purified from *$PhS_3S_3$* pistils through Fast Protein Liquid

Chromatography (FPLC) as described (Entani et al., 2014; Li et al., 2017), recombinant His-PhS$_3$-RNase and -PhS$_3$-RNase (M) were separately used as a substrate for ubiquitination reaction (Li et al., 2017). For immunoblotting, PVDF membranes (Millipore) were probed by primary antibodies, including mouse monoclonal anti-PhS$_3$-RNase, anti-ubiquitin (Abgent), and anti-His (Sigma) antibodies at a 1:2000 dilution, respectively for western blot detection. Image J was used to quantify the immuno signal of the ubiquitinated proteins. K48- or K63-linkage Specific Polyubiquitin Rabbit mAb (Cell Signaling) at a 1:1000 dilution was used to analyze the linkage type of PhS$_3$-RNase ubiquitination.

**Subcellular fractionation and pulse-chase assays**

For subcellular fractionation assay, mature pollen grains of *PhS$_V$S$_V$* were cultured, germinated and collected as described previously (Liu et al., 2014). Style extracts of transgenic pistils containing PhS$_3$-RNase- or PhS$_3$-RNase (M)-FLAG were separately used to incubate the germinated pollen tubes. Then the pollen tubes were harvested for fractionation and equal amounts of protein samples derived from each centrifugation step were applied to immunoblots as described (Liu et al., 2014). For pulse-chase assay, the germinated pollen tubes of *PhS$_V$S$_V$* or *PhS$_3$S$_3$* separately incubated for 1 h with style extracts from the transgenic pistils containing PhS$_3$-RNase- or PhS$_3$-RNase (M)-FLAG were collected and rinsed and allowed to further grow in fresh medium with or without MG132 for about 5 h. Equal amounts of pollen tube samples were loaded and detected by immunoblotting using anti-FLAG antibody (Sigma).

**Cell-free degradation and ubiquitination assays**

Total proteins of germinated *PhS$_V$S$_V$* pollen tubes were extracted on ice using cell-free degradation buffer containing 25 mM Tris-HCl (pH 7.5), 10 mM NaCl, 10 mM MgCl$_2$, 1 mM DTT, 10 mM ATP and 1 mM PMSF. Then equal amounts of extracts were applied to react with recombinant SUMO-His-PhS$_3$-RNase or its -PhS$_3$-RNase (M) with or without MG132 at 30℃. Equal amounts of samples were taken out at indicated time points for immunoblots. Image J was used to quantify the immuno signals. The SUMO-His-tagged fusion proteins were generated as follows. The coding sequences of *PhS$_3$-RNase* (without signal peptide) and *PhS$_3$-RNase* (*M*) were separately

cloned into engineered *pET-30a* (Novagen) containing N-terminal SUMO tag to produce SUMO-His-tagged proteins. Relevant primer sequences are listed in Table S1. The fusion proteins were respectively expressed in *E. coli* Trans BL21 (DE3) plysS (Transgen) at 16℃ for 24 h, and then purified using Ni Sepharose 6 Fast Flow beads. For the cell-free ubiquitination assays, equal amounts of recombinant His-$PhS_3$-RNase and $PhS_3$-RNase (M) were separately incubated with *$PhS_3S_3$* pollen tube extracts using ubiquitin reaction buffer as described previously (Hua and Kao, 2006). Then the His-fused substrates and their ubiquitinated forms were purified from the reaction products through Ni Sepharose 6 Fast Flow beads for immunoblots as described above.

**Pull-down assay**

The coding sequences of *$PhS_3$-RNase* (without signal peptide) and *$PhS_3$-RNase* (*M*) were separately cloned into *pMAl-c2x* (Novagen) to generate MBP-tagged fusion proteins. The full length of *$PhS_{3L}SLF1$* was cloned into engineered *pET-30a* (Novagen) described above to produce SUMO-His-$PhS_{3L}$SLF1. Relevant primer sequences used are listed in Table S1. All the recombinant proteins were induced overnight at 16℃ at 180 rpm, with MBP-tagged proteins expressed in *E. coli* Trans BL21 (DE3) plysS cells described above and SUMO-His-$PhS_{3L}$SLF1 in *E. coli* Trans BL21 (DE3) (Transgen). Cells were collected and resuspended using binding buffer [20 mM Tris-HCl (pH 8.0), 200 mM NaCl, 1 mM DTT and 1 mM EDTA (pH 8.0)] for ultrasonication on ice. Then equal lysates containing SUMO-His-$PhS_{3L}$SLF1 were incubated with the same amount of lysates containing MBP or MBP-tagged fusion protein ($PhS_3$-RNase or its six mutant forms), respectively for 2 h at 4℃. The mixed lysates were subsequently immobilized on Dextrin Sepharose High Performance (GE heathcare, 10284602) following the manufacturer's instructions and eluted by binding buffer supplemented with 10 mM maltose for immunoblots using anti-MBP (NEB) and anti-His (Sigma) antibodies.

**Bimolecular fluorescence complementation (BiFC) and split firefly luciferase complementation (SFLC) assays**

For BiFC assay, the coding sequences of *$PhS_3$-RNase* (without signal peptide) and *$PhS_3$-RNase* (*M*) were separately amplified and inserted into *pSY-735-35S-cYFP-HA* and the full-length cDNA

of *$PhS_{3L}SLF1$* was cloned into *pSY-736-35S-nYFP-EE* as described previously (Li et al., 2018). Relevant primer sequences used are listed in Table S1. Different construct combinations (e.g., *nYFP-$PhS_{3L}SLF1$* and *cYFP-$PhS_3$-RNase*), together with *p19* silencing plasmid, were cotransfected into tobacco leaf epidermal cells by *Agrobacterium* (GV3101)-mediated infiltration to generate fusion proteins (e.g., nYFP-$PhS_{3L}$SLF1 and cYFP-$PhS_3$-RNase) for their interaction test. After being cultured for another 48 h in the dark, a portion of the injected leaf was cut off and subjected to the confocal microscope (Zeiss LSM710) to capture the YFP signal. For the SFLC assay, *$PhS_{3L}SLF1$* (or *$PhS_3SLF1$*) and *$PhS_3$-RNase* (or its mutant forms) were cloned into *pCAMBIA1300-35S-HA-nLUC-RBS* and *pCAMBIA1300-35S-cLUC-RBS* vectors, respectively, as described (Liu et al., 2018). At 48 h post-injection, 1 mM luciferin was sprayed on the injected leaves and the LUC signals captured using a cooled CCD imaging system (Berthold, LB985).

**Aniline blue staining of pollen tubes within pistils**

Pollinated pistils were chemically fixed and treated for observation as described (Liu et al., 2014).

**Results**

**S-RNase polyubiquitination mainly occurs through K48 linkages at three conserved spatial regions among S-RNases**

Previous studies have revealed that S-RNase is ubiquitinated in cross-pollen tubes, but it remains unclear as to the linkage type or site of this ubiquitination. To investigate these questions, we performed an *in vitro* ubiquitination assay and showed that both oligo- and polyubiquitinated $PhS_3$-RNase were detected by anti-ubiquitin, -$PhS_3$-RNase and -ubiquitin-K48 antibodies compared to *$PhS_3S_{3L}$* wild-type control, indicating that non-self $PhS_{3L}$SLF1 are capable of forming $SCF^{SLF}$ complex to ubiquitinate $PhS_3$-RNase mainly through K48-linked polyubiquitin chains (Fig. 1a). To further detect the ubiquitination site of S-RNase, we used LC-MS/MS and identified six ubiquitinated residues at T102, K103, C118, T153, K154 and K217 of $PhS_3$-RNase by wild-type pistils cross-pollinated with the transgenic pollen containing the pollen-specific

*$PhS_{3L}SLF1$* in *P. hybrida* (Fig. 1b and Fig. S1). Furthermore, we found that the ubiquitinated C118, T153, K154 and K217 were exclusively detected in cross-pollinated pistils, suggesting that they are specific for cross-pollination, whereas the ubiquitinated T102 and K103 were detected in both unpollinated and self-pollinated pistils (Fig. S2), suggesting that they likely occur before S-RNase uptake into pollen tubes.

To determine the locations of these ubiquitinated amino acid residues in S-RNases, we compared a total of 36 S-RNases from Solanaceae and found that C118 is within conserved (C) 3 region, T102 and K103 adjacent to hypervariable (Hv) b, T153 and K154 between C4 and C5 and K217 at the C terminal region, implying they are located in three largely conserved S-RNase regions (Fig. 1c and Fig. S3 and Table S2). Next, we reasoned that the ubiquitination sites should be spatially close to E2. To examine this possibility, we determined the spatial localization of six ubiquitinated residues on the predicted spatial structure of $PhS_3$-RNase and found that T102 and K103 are located near the Hvb region on an interface between S-RNase and SLF and termed region (R) I, T153, K154 and K217 in a region close to E2 and termed R II, whereas C118 inside the predicted spatial structure and named as R III (Fig. 1d). Taken together, our results demonstrated that S-RNases are ubiquitinated mainly through K48 linkage at three largely conserved spatial regions among Solanaceae S-RNases.

**Two ubiquitinated amino acids from R I are partially involved in $PhS_3$-RNase degradation during cross-pollination**

To examine how six ubiquitinated amino acids from three spatial regions mediate the S-RNase ubiquitination, we first designed a mutant construct named MI containing T102A and K103R substitutions incapable of ubiquitination at R I of $PhS_3$-RNase and showed that its RNase activity increases with time, similar to wild type (Fig. S4a), suggesting that MI possesses normal ribonuclease activity. To examine whether the substitutions affect the subcellular location of $PhS_3$-RNase, we did fractionation experiments and found that MI is predominantly enriched in the S160 fraction derived from the pollen tube cytosol, similar to wild-type $PhS_3$-RNase ($S_3R$) (Fig.

S4b). Furthermore, we performed pull-down, split firefly luciferase complementation (SFLC) and bimolecular fluorescence complementation (BiFC) assays and found that MI is capable of interacting with non-self $PhS_{3L}$SLF1 (Fig. S4c-e). Nevertheless, we also found that it displayed a weak interaction with self $PhS_3$SLF1 (Fig. S5), similar to previous studies (Kubo et al., 2010; Hua and Kao, 2006). Consistent with these findings, we found that the predicted structure and electrostatic potentials of MI remain essentially unaltered (Fig. S6). Taken together, these results indicated that MI has the enzymatic activity and structure similar to wild-type $S_3$R.

To examine the *in vivo* function of MI, we transformed *$S_3R$* and *MI* driven by the pistil-specific *Chip* promotor into SI *$PhS_3S_{3L}$* plants, respectively and also transformed their *FLAG*-tagged forms into *$PhS_3S_{3L}$*. For each construct, we identified at least 24 $T_0$ transgenic lines by PCR analysis (Fig. S7 and S8) and found that *MI* is expressed normally in the transgenic lines (Fig. S9 and S10a and b). Furthermore, self-pollination assays showed that each construct did not alter the SI phenotypes of the transgenic plants (Table S3 and S4). To examine their roles in cross-pollination, we further identified several lines with similar transgene expression levels. Compared to about 398 seed set per capsule from *$PhS_3S_{3L}$* carrying the transgenic *$S_3R$* (*$S_3S_{3L}$/$S_3R$*-60) pollinated with cross pollen of *$PhS_VS_V$*, *$S_3S_{3L}$/MI* had a reduced seed set of 298 with a reduction of 25% (Fig. S10c and d and Table S3). Consistent with this, we also found a substantial reduction of seed sets derived from cross-pollination of the *FLAG*-tagged transgenic line *$S_3S_{3L}$/MI-FLAG*-24 (292 per capsule) with a 30% reduction compared to 421 seeds per capsule from *$S_3S_{3L}$/$S_3R$-FLAG*-34 (Fig. S10c and d and Table S4). Taken together, these results suggested that the ubiquitinated R I is involved in cross-pollination.

To verify this role, we assessed the degradation rates of recombinant SUMO-His-tagged $S_3$R and MI proteins by cell-free degradation assays using self- (*$PhS_3S_3$*) or cross- (*$PhS_VS_V$*) pollen tube extracts (PTE). The results showed that both SUMO-His-tagged $S_3$R and MI remained essentially stable in *$PhS_3S_3$* PTE but SUMO-His-$S_3$R degraded rapidly in the *$PhS_VS_V$* PTE without MG132 and only 7% remained after 10-minute treatment (Fig. S10e and f). However, the degradation rates slightly decreased and about 25% remained after 10-minute treatment for SUMO-His-MI protein

(Fig. S10f), showing that MI degradation was partially inhibited and thus resulted in its accumulation in cross-pollen tubes. Consistently, both $S_3$R-FLAG and MI-FLAG remained largely stable in self- (*Ph$S_3S_3$*) pollen tubes, but their amounts significantly decreased in cross- (*Ph$S_V S_V$*) pollen tubes during semi *in vivo* pulse-chase experiments using style extracts of *$S_3S_{3L}$*/*MI-FLAG*-24 or *$S_3S_{3L}$*/*$S_3$R-FLAG*-34 to mimic self- and cross-pollination (Fig. S10g). Nevertheless, about 12% more remained for MI-FLAG in cross-pollen tubes compared to $S_3$R-FLAG, suggesting the cross-pollen rejections by the transgenic pistils containing MI-FLAG mainly resulted from its decreased degradation. Besides, degradations of these proteins by cross pollen were significantly delayed by MG132 treatment (Fig. S10e, f and g), indicating the degradation of MI by the UPS pathway similar to wild type.

To confirm the role of the ubiquitinated R I in S-RNase degradation, we further performed ubiquitination assays and found that different from self- (*Ph$S_3S_3$*) PTE, both polyubiquitinated His-tagged $S_3$R and MI proteins were detected by anti-ubiquitin and -His antibodies (Fig. S11 and S12) after incubation with $SCF^{PhS_{3L}SLF1}$ serving as E3, indicating that they both could be specifically ubiquitinated by non-self $SCF^{PhS_{3L}SLF1}$. Nevertheless, the ubiquitinated products of MI reduced to about 60% of $S_3$R (Fig. S11), suggesting that the ubiquitinated residues located in R I are partially responsible for the ubiquitination of Ph$S_3$-RNase by cross pollen. Taken together, these results revealed that two ubiquitinated amino acids from R I are partially involved in Ph$S_3$-RNase degradation during cross-pollination.

**The R II from Ph$S_3$-RNase serves as a major region for its ubiquitination and degradation in cross-pollen tubes**

To examine the function of three ubiquitinated amino acids from R II, we followed a similar strategy to that used for R I by creating MII with T153A, K154R and K217R substitutions of Ph$S_3$-RNase. We found that its RNase activity increases with time, similar to wild type (Fig. 2a), suggesting that it possesses normal ribonuclease activity. Second, it showed that MII is also predominantly located in the pollen tube cytosol (Fig. 2b), capable of interacting with non-self

$PhS_{3L}$SLF1 (Fig. 2c-e), also with a weak interaction with self $PhS_3$SLF1 (Fig. S5) and had unaltered predicted structure and electrostatic potentials (Fig. S6). Furthermore, *MII* and its *FLAG*-tagged transgenes were expressed normally in SI $PhS_3S_{3L}$ plants, and the transgenic lines also maintained SI phenotype (Fig. 2f and g and Fig. S7-9 and Table S3 and S4). Compared to *MI* transgenic lines, a significant difference observed for $S_3S_{3L}$/*MII* was the seed sets derived from pollination with cross pollen of $PhS_VS_V$ (ca. 75 seed sets per capsule), with a significant reduction of 81% compared with $S_3S_{3L}$/$S_3R$-60 (398 seed sets per capsule) (Fig. 2h and Fig. S13a and Table S3). Consistent with this, compared to 421 seeds per capsule from $S_3S_{3L}$/$S_3R$-*FLAG*-34, about 113 seeds were set for the *FLAG*-tagged transgenic lines with a significant 73% reduction (Fig. 2h and Fig. S13b and Table S4). We further found that the *MII-FLAG* transgene leads to much less seed set per capsule than *MI-FLAG* when their protein levels remain similar (Fig. 2g and h and Fig. S13b), indicating that the ubiquitinated R II plays a major role in cross-pollination. Furthermore, cell-free degradation assays and pulse-chase experiments mimicking cross-pollination showed that the degradation of MII protein mainly through the UPS pathway is severely inhibited, with a significantly decreased difference between its remaining amounts in self- and cross-pollen tubes compared with MI (Fig. 2i and j and Fig. S10f). Consistently, *in vitro* ubiquitination assays showed that the ubiquitination amount of MII with $SCF^{PhS_{3L}SLF1}$ serving as E3 significantly reduced to 40% of $S_3$R, with a reduction of 20% compared with MI (Fig. S11). In addition, both the attenuated degradation and ubiquitination of MII specifically occurred in cross-pollen tubes (Fig. 2i and j and Fig. S11 and S12). Taken together, these results suggested that R II of $PhS_3$-RNase acts as a major ubiquitination region for its degradation resulting in cross-pollination.

**K154 and K217 from R II act as two major ubiquitination residues for $PhS_3$-RNase degradation in cross-pollen tubes**

To explore the function of three lysines (K103, K154 and K217) and two threonines (T102 and T153) residues of $PhS_3$-RNase in its degradation, we designed two mutant constructs termed MK (K103R, K154R and K217R) and MT (T102A and T153A), which showed similar enzymatic

activities, subcellular localizations, SLF interactions, predicted structures and electrostatic potentials to wild-type $S_3$R as well as normal pistil expressions and SI phenotypes similar to SI *PhS$_3$S$_{3L}$* plants (Fig. 3a-g and Fig. S5-9 and Table S3 and S4). However, *MK* and *MT* transgenic lines showed differential seed sets of 207 and 356 per capsule after pollination with cross pollen of *PhS$_V$S$_V$*, with a significant reduction of 48% and 15%, respectively, compared with *S$_3$S$_{3L}$/S$_3$R*-60 (398 seeds per capsule) (Fig. 3h and Fig. S14a and Table S3), consistent with that *S$_3$S$_{3L}$/MK-FLAG*-16 set 113 seeds per capsule with a significant reduction of 73% and 66% compared with *S$_3$S$_{3L}$/S$_3$R-FLAG*-34 (421 seeds per capsule) and *S$_3$S$_{3L}$/MT-FLAG*-44 (334 seeds per capsule), respectively (Fig. 3h and Fig. S14b and Table S4). In addition, we showed that compared with *MT* transgene, *MK* resulted in more seed set reduction similar to *MII* when the transgene expression levels were similar (Fig. 3g and h), suggesting that the identified lysine amino acids, especially K154 and K217, play a major role in the ubiquitination and degradation of $PhS_3$-RNase. Furthermore, cell-free degradation and pulse-chase assays showed that MK degradation by the 26S proteasome in cross- (*PhS$_V$S$_V$*) pollen tubes had been significantly delayed compared with MT in the absence of MG132 (Fig. 3i and Fig. S14c and d). Ubiquitination assays also indicated that the lysine residues rather than threonine act as the major sites for the $PhS_3$-RNase ubiquitination by non-self $SCF^{PhS_{3L}SLF1}$ (Fig. 3j and Fig. S12). Taken together, our results suggested that K154 and K217 from R II function as two major ubiquitination residues of $PhS_3$-RNase for cross-pollination.

**R III functions as the second major ubiquitination region for $PhS_3$-RNase degradation allowing cross-pollination**

To investigate the function of the ubiquitination site C118 from the internal R III, we designed MIII (C118A) and found that it also maintains ribonuclease activity, subcellular localization and predicted structure similar to wild-type $S_3$R (Fig. S5, S6 and S15). We further transformed *MIII* and its *FLAG*-tagged form into SI *PhS$_3$S$_{3L}$* plants and detected significantly reduced seed sets of about 160 and 261 per capsule from *S$_3$S$_{3L}$/MIII*-84 and *S$_3$S$_{3L}$/MIII-FLAG*-18 after pollination with

cross pollen of *PhS$_V$S$_V$*, with a respective reduction of 59% and 38% compared with *S$_3$S$_{3L}$*/*S$_3$R*-60 and *S$_3$S$_{3L}$*/*S$_3$R-FLAG*-34 (Fig. S7-9 and S16a-d and Table S3 and S4). Furthermore, the average seed set per capsule was much less than *S$_3$S$_{3L}$*/*MI-FLAG* when they showed similar transgene expression levels (Fig. S16b and d), supporting a role of R III in the degradation of PhS$_3$-RNase. Besides, we detected a marked accumulation of MIII in cross-pollen tubes compared with S$_3$R and MI in the absence of MG132 (Fig. S10e-g and S16e, f) and a significantly decreased ubiquitination amount by non-self SCF$^{PhS_{3L}SLF1}$ compared with MI (Fig. S11 and S12). Taken together, these results suggested that the R III acts as a second major ubiquitination region for the degradation of PhS$_3$-RNase, thus leading to cross-pollination.

**R I, II and III of PhS$_3$-RNase function additively in its degradation during cross-pollination**

To examine the function of the three ubiquitination regions together, we made MI/II/III (T102A, K103R, T153A, K154R, K217R and C118A). Similar to wild-type PhS$_3$-RNase, the mutant form exhibited normal physicochemical properties (Fig. S5, S6 and S17) but resulted in 197 and 93 cross seeds per capsule derived from *S$_3$S$_{3L}$*/*MI*/*II*/*III*-45 and *S$_3$S$_{3L}$*/*MI*/*II*/*III-FLAG*-49 with pollen of *PhS$_V$S$_V$*, respectively, a significant reduction of 50% and 77% similar to the lines containing the mutated R II (Fig. 4a-c and Fig. S7-9 and S18 and Table S3 and S4). Furthermore, the degradation of MI/II/III in cross-pollen tubes was strongly inhibited in the absence of MG132 (Fig. 4d and e), indicating a significantly reduced ubiquitination by non-self SCF$^{PhS_{3L}SLF1}$ in cross-pollen (Fig. 4f and Fig. S12). Taken together, these results suggested that the degradation of PhS$_3$-RNase is largely dependent on an additive role of its three ubiquitination regions during cross-pollination.

**Discussion**

Previous studies have shown that non-self S-RNases are collaboratively recognized by multiple non-self SLFs leading to the formation of canonical SCF$^{SLF}$ complexes for their ubiquitination and subsequent degradation by the 26S proteasome during cross-pollination, but the ubiquitination

linkage type and site remain unclear. In this study, we found that non-self S-RNase is mainly polyubiquitinated through K48 linkages by $SCF^{SLF}$ at three spatial regions (R I, II and III) in *P. hybrida*. Among them, R I ubiquitination appears to occur before S-RNase uptake into pollen tubes with a minor role, if any, in cross-pollen tubes, whereas R II and III act as two major ubiquitination regions for S-RNase degradation. Consistently, Hua and Kao (2008) identified six lysine residues mainly responsible for the ubiquitination and degradation of $S_3$-RNase in *P. inflata*, which are located in the same region of R II identified in our study, reinforcing the major role of R II in *Petunia* $S_3$-RNase degradation for cross-pollination. Based on our results, we propose a stepwise UPS model for S-RNases cytotoxicity restriction allowing cross-pollination in *P. hybrida* (Fig. 5). In this model, both self and non-self S-RNases with a small fraction of R I ubiquitinated forms likely mediated by an unknown E3 ligase are taken up into the cytosols of either self- or cross-pollen tubes. Firstly, the R I ubiquitinated forms would make them unable to be recognized by SLFs but degraded by the 26S proteasome. Secondly, other S-RNases could be recognized by SLFs on the basis of 'like charges repel and unlike charges attract', and the like electrostatic potentials together with other unknown forces between self S-RNase and its cognate SLF would result in the formation of non-functional $SCF^{SLF}$ complexes as demonstrated previously (Li et al., 2017). In contrast, non-self S-RNase would be attracted by unlike electrostatic potentials and other unknown factors and polyubiquitinated by functional $SCF^{SLF}$ complexes (Li et al., 2017; Sun and Kao, 2018) at R II, leading to its degradation by the 26S proteasome. Thirdly, the internal R III of non-self S-RNase could be exposed by a conformational change for its further ubiquitination by SLFs and degradation resulting in cross-pollination. Our studies have revealed that the ubiquitination and degradation of non-self S-RNases depend on at least three regions with distinct ubiquitination sites, including lysine, threonine and cysteine, reinforcing the notion that the restriction of S-RNase cytotoxicity occurs mainly by the ubiquitination-mediated degradation mechanism in *P. hybrida* (Liu et al., 2014).

Nevertheless, the underlying mechanisms of R I and III ubiquitination remain to be further elucidated. Notably, newly synthesized secretory proteins are constantly scrutinized and destructed by the protein quality control system such as ER-associated degradation (ERAD) or autophagy to

maintain proteostasis once they are misfolded or aggregated (Anelli and Sitia, 2008). The ubiquitination of R I in the unpollinated pistils suggested that it might result from the polyubiquitination of misfolded $PhS_3$-RNases. Ubiquitination of closely spaced residues is predicted to be important for polyubiquitin chain assembly (Wang et al., 2012). Here, we found that the identified threonine ubiquitination residues paired with lysine also contribute to the ubiquitination and degradation of non-self S-RNase for cross-pollination, suggesting that they may play a role in building polyubiquitin chains long enough for proteasome recognition (Thrower et al., 2000). In addition, ubiquitin often serves as a critical signal governing the membrane traffic system. Monoubiquitination is sufficient to initiate the internalization of plasma membrane proteins, and K63-linked polyubiquitination is frequently involved in their subsequent sorting and trafficking (Hicke and Dunn, 2003; Clague and Urbé, 2010; Paez Valencia et al., 2016). It is thus possible that R I could also be monoubiquitinated leading to S-RNase entry into pollen tubes by endocytosis, consistent with the results showing that a small fraction of S-RNases is sequestered in microsome fractions (Liu et al., 2014). As for the internal R III, its ubiquitination likely occurs only after being exposed. Therefore, the ubiquitination of R II might lead to the conformational change of non-self S-RNase and exposure of R III, and the subsequent ubiquitination of R III would further block the enzymatic activity of the S-RNase (Sagar et al., 2007). Previous simulations demonstrated that the conserved complementary electrostatic patterns and hydrophobic patches of Rpn10, a recognition subunit of proteasome, and K48-linked tetraubiquitin of the substrates are critical for their interaction (Zhang et al., 2016). Likewise, the ubiquitination of R III might further enhance the electrostatic potentials and hydrophobicity to strengthen the recognition of ubiquitinated S-RNase by the proteasome as well as its degradation.

It remains unclear why the additive action of the three regions did not completely restrict non-self S-RNase cytotoxicity in cross-pollen tubes. We suggest that there might be additional mechanism (s) occurring either after the R III-mediated ubiquitination of non-self S-RNase or during S-RNase uptake into pollen tubes by endocytosis resulting in its compartmentalization (Goldraij et al., 2006). In *Nicotiana*, S-RNases appeared to be sequestered early in vacuole but released out late to the cytosol in self-pollen tubes (Goldraij et al., 2006). In *P. hybrida*, a small

amount of S-RNases was detected in the microvesicles of pollen tubes (Liu et al., 2014). Furthermore, it showed that S-RNases were compartmentalized in the cross-pollen tubes even 36 hours after cross-pollination in *Nicotiana* (Goldraij et al., 2006), longer than 24h, the longest post-pollination time used for identification of R I/II/III ubiquitination in *P. hybrida*. Together, these findings suggest that S-RNase compartmentalization and its stepwise ubiquitination and degradation might function synergistically from the beginning to the late phases of S-RNase action in the cross-pollen tubes. In this scenario, it's possible that the mutant S-RNase evading ubiquitination and degradation would partially reverse the downstream response derived from non-self recognition between SLFs and S-RNases to that of their self- recognition, further leading to S-RNase release from the vacuole to varying degrees similar to the late stage of self-pollen rejection proposed in *Nicotiana* (Goldraij et al., 2006). In this view, the increased S-RNase cytotoxicity could result from the total impacts of S-RNases both originally present in and later released from the vacuole into the cross-pollen tube cytosols. Nevertheless, removal of the additive ubiquitination of R I/II/III could not lead to sufficient cytosolic S-RNases, thus allowing the cross-pollen escape and seed sets. Further investigation into the S-RNase uptake mechanism and the relationship between the stepwise ubiquitination and degradation of S-RNases and their compartmentalization would provide the answer to these possibilities.

T2 RNases are widespread in every organism except Archaea and involved in a variety of biological processes, including phosphate starvation, viral infection, self-fertilization, tumor growth control and cell death (Löffler et al., 1992; Bariola et al., 1994; Meyers et al., 1999; Thompson and Parker, 2009; Ramanauskas and Igić, 2017). However, our understanding of their functions remains largely incomplete, especially when their roles appear to be independent of their enzymatic activity. In *Saccharomyces cerevisiae*, T2 RNase Rny1 can be released from the vacuole to cleave tRNA and rRNA under super oxygen stress (Thompson and Parker, 2009). Rny1 is indispensable for cell viability, but overexpressed Rny1 can act as a cytotoxin during oxidative stress (MacIntosh et al., 2001; Thompson and Parker, 2009). Moreover, its inactivation strikingly has no effects on cell viability (MacIntosh et al., 2001), but the underlying mechanism remains elusive. In human, RNASET2 is not only implicated to regulate neurodevelopment downstream

immune response but also serve as a tumor suppresser (Henneke et al., 2009), whereas how it contributes to this process in a cleavage-independent manner is poorly defined. In addition, the catalytic-independent function of T2 RNase has also been confirmed for ACTIBIND from *Aspergillus niger* that can bind to and destroy the normal actin networks, which is supposed to be conserved in other T2 RNase family members including S-RNases (Roiz et al., 2006). Thus, T2 RNase may act as a molecular signal mediating multiple biological settings, revealing that diverse T2 RNase roles could be derived through neofunctionalization in these lineages.

In S-RNase-based SI, Yang et al. (2018) reported an S-RNase-mediated actin disruption in apple (*Malus*×*domestica*). The disrupted cytoskeleton dynamic serves as a major cause of PCD (Thomas et al., 2006), which is also proposed to occur in self-pollen tubes of *Pyrus bretschneideri* (Chen et al., 2018). Moreover, self S-RNase can disrupt $Ca^{2+}$ gradient at pollen tube apex through inhibiting phospholipase C (PLC) (Qu et al., 2017). Besides, heat-inactivated S-RNase surprisingly exerts a more severe inhibition of pollen tubes (Gray et al., 1991). These studies suggest that S-RNase could function in a signaling pathway independent of its enzymatic activity. Our results indicated that self S-RNase could be partially ubiquitinated extracellularly and destroyed during its uptake, but we can not rule out the possibility that its ubiquitination could act as an initial signal for SI response.

In addition to ubiquitination, a recent study in *Solanum chacoense* showed that the number of carbohydrate chains of S-RNase may influence its threshold for pollen rejection (Liu et al., 2008). Torres-Rodriguez et al. (2020) found that the ribonuclease activity of $S_{C10}$-RNase could be significantly enhanced if its conserved Cys155-Cys185 disulphide bond was reduced by *Nicotiana alata* thioredoxin type h (Natrxh) in the pollen tube cytosols. Furthermore, the disulphide bond of $S_{C10}$-RNase is highly conserved among S-RNases (Anderson et al., 1989), and it is likely that S-RNase reduction occurs after an incompatible recognition between SLFs and S-RNases leading to RNA degradation necessary for self-pollen rejection. In this case, the mutant S-RNases incapable of ubiquitination and degradation in the cytosols of cross-pollen tubes could induce the downstream responses including S-RNase reduction, resulting in its increased ribonuclease

activity as well as cytotoxicity for cross-pollen inhibition. Moreover, as phosphorylation serves as a critical modification modulating multiple cellular events, it may also be involved in S-RNase activity regulation and the downstream signaling transduction in Solanaceae-type SI. Besides, previous studies have shown that there should exist other factors except electrostatic potentials that contribute to the recognition between SLF and S-RNase (Li et al., 2017). Thus, future studies on the structure of SLF bound to S-RNase, other post-translational modifications such as glycosylation, reduction and phosphorylation of S-RNase and their relationships with its ubiquitination should shed light on how S-RNase functions and stimulates downstream signaling networks in the pollen tubes.

In conclusion, our results have revealed a novel stepwise UPS mechanism for S-RNase cytotoxicity restriction resulting in cross-pollination in *P. hybrida*. Our findings also indicate a possible mechanism for dynamic regulation of secreted cytotoxin activities including other T2 ribonuclease members. Further validation of this mechanism using biochemical and cytological approaches is expected to provide additional insights into UPS and Solanaceae-type SI.

**Acknowledgments**

This work was supported by the Strategic Priority Research Program of the Chinese Academy of Sciences (XDB27010302) and the National Natural Science Foundation of China (32030007).

**Author contributions**

Y.X conceived and designed the project. H.Z. and Y.S. performed the experiments. J.L. and Yue Zhang conducted functional analyses of *$PhS_{3L}SLF1$*. H.H. assisted transgenic plant construction. Q.L. and Yu'e Zhang provided technical support. H.Z. and Y.X. analyzed data and wrote the manuscript. All authors commented on the article. HZ and YS contributed equally to this work.

**Data availability**

The data supporting the findings of this work are available from the corresponding author upon request.

**References**

**Anderson, M.A., Cornish, E.C., Mau, S.L., Williams, E.G., Hoggart, R., Atkinson, A., Bonig, I., Grego, B., Simpson, R., and Roche, P.J. 1986.** Cloning of cDNA for a stylar glycoprotein associated with expression of self-incompatibility in *Nicotiana alata*. *Nature* **321,** 38-44.

**Anderson, M.A., McFadden, G.I., Bernatzky, R., Atkinson, A., Orpin, T., Dedman, H., Tregear, G., Fernley, R., and Clarke, A.E. 1989.** Sequence variability of three alleles of the self-incompatibility gene of *Nicotiana alata*. *Plant Cell* **1**, 483-491.

**Anelli, T., and Sitia, R. 2008.** Protein quality control in the early secretory pathway. *The EMBO Journal* **27**, 315-327.

**Baker, N.A., Sept, D., Joseph, S., Holst, M.J., and McCammon, J.A. 2001.** Electrostatics of nanosystems: application to microtubules and the ribosome. *Proceedings of the National Academy of Sciences*, *USA* **98**, 10037-10041.

**Bariola, P.A., Howard, C.J., Taylor, C.B., Verburg, M.T., Jaglan, V.D., and Green, P.J. 1994.** The Arabidopsis ribonuclease gene RNS1 is tightly controlled in response to phosphate limitation. *Plant Journal* **6**, 673-685.

**Chen, J., Wang, P., de Graaf, B.H.J., Zhang, H., Jiao, H., Tang, C., Zhang, S., and Wu, J. 2018.** Phosphatidic acid counteracts S-RNase signaling in pollen by stabilizing the actin cytoskeleton. *Plant Cell* **30**, 1023-1039.

**Clague, M.J., and Urbé, S. 2010.** Ubiquitin: same molecule, different degradation pathways. *Cell* **143**, 682-685.

**De Nettancourt, D. 2001.** Incompatibility and incongruity in wild and cultivated plants. Berlin: Springer Verlag. doi: 10.1007/978-3-662-04502-2

**Entani, T., Kubo, K.-I., Isogai, S., Fukao, Y., Shirakawa, M., Isogai, A., and Takayama, S. 2014.** Ubiquitin-proteasome-mediated degradation of S-RNase in a Solanaceous cross-compatibility reaction. *Plant Journal* **78**, 1014-1021.

**Foote, H.C., Ride, J.P., Franklin-Tong, V.E., Walker, E.A., Lawrence, M.J., and Franklin, F.C. 1994.** Cloning and expression of a distinctive class of self-incompatibility (*S*) gene from *Papaver rhoeas* L. *Proceedings of the National Academy of Sciences*, *USA* **91**, 2265-2269.

**Franklin-Tong, V.E. 2008.** Self-incompatibility in flowering plants. Springer, Berlin Heidelberg.

**Fujii, S., Kubo, K.-I., and Takayama, S. 2016.** Non-self- and self-recognition models in plant self-incompatibility. *Nature Plants* **2**, 16130.

**Goldraij, A., Kondo, K., Lee, C.B., Hancock, C.N., Sivaguru, M., Vazquez-Santana, S., Kim, S., Phillips, T.E., Cruz-Garcia, F., and McClure, B. 2006.** Compartmentalization of S-RNase and HT-B degradation in self-incompatible *Nicotiana*. *Nature* **439**, 805-810.

**Gray, J.E., McClure, B.A., Bonig, I., Anderson, M.A., and Clarke, A.E. 1991.** Action of the style product of the self-incompatibility gene of *Nicotiana alata* (S-RNase) on in vitro-grown pollen tubes. *Plant Cell* **3**, 271-283.

**Henneke, M., Diekmann, S., Ohlenbusch, A., Kaiser, J., Engelbrecht, V., Kohlschütter, A., Krätzner, R., Madruga-Garrido, M., Mayer, M., Opitz, L., *et al.* 2009.** RNASET2-deficient cystic leukoencephalopathy resembles congenital cytomegalovirus brain infection. *Nature Genetics* **41**, 773-775.

**Hicke, L., and Dunn, R. 2003.** Regulation of membrane protein transport by ubiquitin and ubiquitin-binding proteins. *Annual Review of Cell and Developmental Biology* **19**, 141-172.

**Hua, Z., Fields, A., and Kao, T.-H. 2008.** Biochemical models for S-RNase-based self-incompatibility. *Molecular plant* **1**, 575-585.

**Hua, Z., and Kao, T.-H. 2006.** Identification and characterization of components of a putative *Petunia S*-locus F-box-containing E3 ligase complex involved in S-RNase-based self-incompatibility. *Plant Cell* **18**, 2531-2553.

**Hua, Z., and Kao, T.-H. 2008.** Identification of major lysine residues of $S_3$-RNase of *Petunia inflata* involved in ubiquitin-26S proteasome-mediated degradation *in vitro*. *Plant Journal* **54**, 1094-1104.

**Huang, J., Zhao, L., Yang, Q., and Xue, Y. 2006.** AhSSK1, a novel SKP1-like protein that interacts with the *S*-locus F-box protein SLF. *Plant Journal* **46**, 780-793.

**Kakita, M., Murase, K., Iwano, M., Matsumoto, T., Watanabe, M., Shiba, H., Isogai, A., and Takayama, S. 2007.** Two distinct forms of M-locus protein kinase localize to the plasma membrane and interact directly with *S*-locus receptor kinase to transduce self-incompatibility signaling in *Brassica rapa*. *Plant Cell* **19**, 3961-3973.

**Kubo, K.-I., Entani, T., Takara, A., Wang, N., Fields, A.M., Hua, Z., Toyoda, M., Kawashima, S.-I., Ando, T., Isogai, A., *et al.* 2010.** Collaborative non-self recognition system in S-RNase-based self-incompatibility. *Science* **330**, 796-799.

**Löffler, A., Abel, S., Jost, W., Beintema, J.J., and Glund, K. 1992.** Phosphate-regulated induction of intracellular ribonucleases in cultured tomato (*Lycopersicon esculentum*) cells. *Plant Physiology* **98**, 1472-1478.

**Lai, Z., Ma, W., Han, B., Liang, L., Zhang, Y., Hong, G., and Xue, Y. 2002.** An F-box gene linked to the self-incompatibility (*S*) locus of *Antirrhinum* is expressed specifically in pollen and tapetum. *Plant Molecular Biology* **50**, 29-42.

**Lee, H.S., Huang, S., and Kao, T.-H. 1994.** *S* proteins control rejection of incompatible pollen in *Petunia inflata*. *Nature* **367**, 560-563.

**Li, J., Zhang, Y., Song, Y., Zhang, H., Fan, J., Li, Q., Zhang, D., and Xue, Y. 2017.** Electrostatic potentials of the *S*-locus F-box proteins contribute to the pollen *S* specificity in self-incompatibility in *Petunia hybrida*. *Plant Journal* **89**, 45-57.

**Li, S., Tian, Y., Wu, K., Ye, Y., Yu, J., Zhang, J., Liu, Q., Hu, M., Li, H., Tong, Y., *et al.* 2018.** Modulating plant growth-metabolism coordination for sustainable agriculture. *Nature* **560**, 595-600.

**Li, W., and Chetelat, R.T. 2014.** The role of a pollen-expressed cullin1 protein in gametophytic self-incompatibility in *Solanum*. *Genetics* **196**, 439-442.

**Liang, M., Cao, Z., Zhu, A., Liu, Y., Tao, M., Yang, H., Xu, Q., Jr., Wang, S., Liu, J., Li, Y., *et al.* 2020.** Evolution of self-compatibility by a mutant $S_m$-RNase in citrus. *Nature Plants* **6**, 131-142.

**Liu, B., Morse, D., and Cappadocia, M. 2008.** Glycosylation of S-RNases may influence pollen rejection thresholds in *Solanum chacoense*. *Journal of Experimental Botany* **59**, 545-552.

**Liu, Q., Han, R., Wu, K., Zhang, J., Ye, Y., Wang, S., Chen, J., Pan, Y., Li, Q., Xu, X., *et al.* 2018.** G-protein βγ subunits determine grain size through interaction with MADS-domain transcription factors in rice. *Nature Communications* **9**, 852.

**Liu, W., Fan, J., Li, J., Song, Y., Li, Q., Zhang, Y.e., and Xue, Y. 2014.** $SCF^{SLF}$-mediated cytosolic degradation of S-RNase is required for cross-pollen compatibility in S-RNase-based self-incompatibility in *Petunia hybrida*. *Frontiers in Genetics* **5**, 228.

**Livak, K.J., and Schmittgen, T.D. 2001.** Analysis of relative gene expression data using real-time quantitative PCR and the 2(-Delta Delta C(T)) Method. *Methods* **25**, 402-408.

**Ma, R., Han, Z., Hu, Z., Lin, G., Gong, X., Zhang, H., Nasrallah, J.B., and Chai, J. 2016.** Structural basis for specific self-incompatibility response in *Brassica*. *Cell Research* **26**, 1320-1329.

**MacIntosh, G.C., Bariola, P.A., Newbigin, E., and Green, P.J. 2001.** Characterization of Rny1, the Saccharomyces cerevisiae member of the T2 RNase family of RNases: unexpected functions for ancient enzymes? *Proceedings of the National Academy of Sciences*, *USA* **98**, 1018-1023.

**McClure, B. (2009).** Darwin's foundation for investigating self-incompatibility and the progress toward a physiological model for S-RNase-based SI. *Journal of Experimental Botany* **60**, 1069-1081.

**Mcclure, B., Cruz-García, F., and Romero, C. 2011.** Compatibility and incompatibility in S-RNase-based systems. *Annals of Botany* **108**, 647-658.

**McClure, B.A., Haring, V., Ebert, P.R., Anderson, M.A., Simpson, R.J., Sakiyama, F., and Clarke, A.E. 1989.** Style self-incompatibility gene products of *Nicotiana alata* are ribonucleases. *Nature* **342**, 955-957.

**Meyers, G., Saalmüller, A., and Büttner, M. 1999.** Mutations abrogating the RNase activity in glycoprotein $E^{rns}$ of the pestivirus classical swine fever virus lead to virus attenuation. *Journal of Virology* **73**, 10224-10235.

**Paez Valencia, J., Goodman, K., and Otegui, M.S. 2016.** Endocytosis and endosomal trafficking in plants. *Annual Review of Plant Biology* **67**, 309-335.

**Qiao, H., Wang, F., Zhao, L., Zhou, J., Lai, Z., Zhang, Y., Robbins, T.P., and Xue, Y. 2004a.** The F-box protein AhSLF-$S_2$ controls the pollen function of S-RNase-based self-incompatibility. *Plant Cell* **16**, 2307-2322.

**Qiao, H., Wang, H., Zhao, L., Zhou, J., Huang, J., Zhang, Y., and and Xue, Y. 2004b.** The F-box protein AhSLF-$S_2$ physically interacts with S-RNases that may be inhibited by the ubiquitin/26S proteasome pathway of protein degradation during compatible pollination in *Antirrhinum*. *Plant Cell* **16**, 582-595.

**Qu, H., Guan, Y., Wang, Y., and Zhang, S. 2017.** PLC-mediated signaling pathway in pollen tubes regulates the gametophytic self-incompatibility of *Pyrus* species. *Frontiers in Plant Science* **8**, 1164.

**Ramanauskas, K., and Igić, B. 2017.** The evolutionary history of plant T2/S-type ribonucleases. *PeerJ* **5**, e3790.

**Robbins, T.P., Harbord, R.M., Sonneveld, T., and Clarke, K. 2000.** The molecular genetics of self-incompatibility in *Petunia hybrida*. *Annals of Botany* **85**, 105-112.

**Roiz, L., Smirnoff, P., Bar-Eli, M., Schwartz, B., and Shoseyov, O. 2006.** ACTIBIND, an actin-binding fungal T2-RNase with antiangiogenic and anticarcinogenic characteristics. *Cancer* **106**, 2295-2308.

**Sagar, G.D.V., Gereben, B., Callebaut, I., Mornon, J.-P., Zeöld, A., da Silva, W.S., Luongo, C., Dentice, M., Tente, S.M., Freitas, B.C.G., *et al.* 2007.** Ubiquitination-induced conformational change within the deiodinase dimer is a switch regulating enzyme activity. *Molecular and Cellular Biology* **27**, 4774-4783.

**Samuel, M.A., Chong, Y.T., Haasen, K.E., Aldea-Brydges, M.G., Stone, S.L., and Goring, D.R. 2009.** Cellular pathways regulating responses to compatible and self-incompatible

pollen in *Brassica* and Arabidopsis stigmas intersect at Exo70A1, a putative component of the exocyst complex. *Plant Cell* **21**, 2655-2671.

**Samuel, M.A., Mudgil, Y., Salt, J.N., Delmas, F., Ramachandran, S., Chilelli, A., and Goring, D.R. 2008.** Interactions between the S-domain receptor kinases and AtPUB-ARM E3 ubiquitin ligases suggest a conserved signaling pathway in Arabidopsis. *Plant Physiology* **147**, 2084-2095.

**Sassa, H., Nishio, T., Kowyama, Y., Hirano, H., Koba, T., and Ikehashi, H. 1996.** Self-incompatibility (*S*) alleles of the Rosaceae encode members of a distinct class of the T2/S ribonuclease superfamily. *Molecular & General Genetics* : *MGG* **250**, 547-557.

**Schopfer, C.R., Nasrallah, M.E., and Nasrallah, J.B. 1999.** The male determinant of self-incompatibility in *Brassica*. *Science* **286**, 1697-1700.

**Sijacic, P., Wang, X., Skirpan, A.L., Wang, Y., Dowd, P.E., McCubbin, A.G., Huang, S., and Kao, T.-H. 2004.** Identification of the pollen determinant of S-RNase-mediated self-incompatibility. *Nature* **429**, 302-305.

**Sims, T.L., and Ordanic, M. 2001.** Identification of a S-ribonuclease-binding protein in *Petunia hybrida*. *Plant Molecular Biology* **47**, 771-783.

**Sun, L., and Kao, T.-H. 2018.** CRISPR/Cas9-mediated knockout of PiSSK1 reveals essential role of S-locus F-box protein-containing SCF complexes in recognition of non-self S-RNases during cross-compatible pollination in self-incompatible *Petunia inflata*. *Plant Reproduction* **31**, 129-143.

**Suzuki, G., Kai, N., Hirose, T., Fukui, K., Nishio, T., Takayama, S., Isogai, A., Watanabe, M., and Hinata, K. 1999.** Genomic organization of the *S* locus: identification and characterization of genes in SLG/SRK region of $S^9$ haplotype of *Brassica campestris* (syn. *rapa*). *Genetics* **153**, 391-400.

**Takasaki, T., Hatakeyama, K., Suzuki, G., Watanabe, M., Isogai, A., and Hinata, K. 2000.** The S receptor kinase determines self-incompatibility in *Brassica* stigma. *Nature* **403**, 913-916.

**Takayama, S., and Isogai, A. 2005.** Self-incompatibility in plants. *Annual Review of Plant*

*Biology* **56**, 467-489.

**Takayama, S., Shiba, H., Iwano, M., Shimosato, H., Che, F.-S., Kai, N., Watanabe, M., Suzuki, G., Hinata, K., and Isogai, A. 2000.** The pollen determinant of self-incompatibility in *Brassica campestris*. *Proceedings of the National Academy of Sciences*, *USA* **97**, 1920.

**Thomas, S.G., and Franklin-Tong, V.E. 2004.** Self-incompatibility triggers programmed cell death in *Papaver* pollen. *Nature* **429**, 305-309.

**Thomas, S.G., Huang, S., Li, S., Staiger, C.J., and Franklin-Tong, V.E. 2006.** Actin depolymerization is sufficient to induce programmed cell death in self-incompatible pollen. *The Journal of Cell Biology* **174**, 221-229.

**Thompson, D.M., and Parker, R. 2009.** The RNase Rny1p cleaves tRNAs and promotes cell death during oxidative stress in *Saccharomyces cerevisiae*. *The Journal of Cell Biology* **185**, 43-50.

**Thrower, J.S., Hoffman, L., Rechsteiner, M., and Pickart, C.M. 2000.** Recognition of the polyubiquitin proteolytic signal. *The EMBO Journal* **19**, 94-102.

**Torres-Rodriguez, M.D., Cruz-Zamora, Y., Juarez-Diaz, J.A., Mooney, B., McClure, B.A., and Cruz-Garcia, F. 2020.** NaTrxh is an essential protein for pollen rejection in *Nicotiana* by increasing S-RNase activity. *Plant Journal* **103**, 1304-1317.

**Udeshi, N.D., Mertins, P., Svinkina, T., and Carr, S.A. 2013a.** Large-scale identification of ubiquitination sites by mass spectrometry. *Nature Protocols* **8**, 1950-1960.

**Udeshi, N.D., Svinkina, T., Mertins, P., Kuhn, E., Mani, D.R., Qiao, J.W., and Carr, S.A. 2013b.** Refined preparation and use of anti-diglycine remnant (K-ε-GG) antibody enables routine quantification of 10,000s of ubiquitination sites in single proteomics experiments. *Molecular & Cellular Proteomics* **12**, 825-831.

**Ushijima, K., Sassa, H., Dandekar, A.M., Gradziel, T.M., Tao, R., and Hirano, H. 2003.** Structural and transcriptional analysis of the self-incompatibility locus of almond: identification of a pollen-expressed F-box gene with haplotype-specific polymorphism. *Plant Cell* **15**, 771-781.

**Wang, X., Herr, R.A., and Hansen, T.H. 2012.** Ubiquitination of substrates by esterification. *Traffic* **13**, 19-24.

**Wheeler, M.J., de Graaf, B.H.J., Hadjiosif, N., Perry, R.M., Poulter, N.S., Osman, K., Vatovec, S., Harper, A., Franklin, F.C.H., and Franklin-Tong, V.E. 2009.** Identification of the pollen self-incompatibility determinant in *Papaver rhoeas*. *Nature* **459**, 992-995.

**Wiederstein, M., and Sippl, M.J. 2007.** ProSA-web: interactive web service for the recognition of errors in three-dimensional structures of proteins. *Nucleic Acids Research* **35**, W407-410.

**Wilkins, K.A., Poulter, N.S., and Franklin-Tong, V.E. 2014.** Taking one for the team: self-recognition and cell suicide in pollen. *Journal of Experimental Botany* **65**, 1331-1342.

**Willard, L., Ranjan, A., Zhang, H., Monzavi, H., Boyko, R.F., Sykes, B.D., and Wishart, D.S. 2003.** VADAR: a web server for quantitative evaluation of protein structure quality. *Nucleic Acids Research* **31**, 3316-3319.

**Xu, C., Li, M., Wu, J., Guo, H., Li, Q., Zhang, Y.e., Chai, J., Li, T., and Xue, Y. 2013.** Identification of a canonical $SCF^{SLF}$ complex involved in S-RNase-based self-incompatibility of *Pyrus* (Rosaceae). *Plant Molecular Biology* **81**, 245-257.

**Xue, Y., Carpenter, R., Dickinson, H.G., and Coen, E.S. 1996.** Origin of allelic diversity in *Antirrhinum S* locus RNases. *Plant Cell* **8**, 805-814.

**Yang, J., Yan, R., Roy, A., Xu, D., Poisson, J., and Zhang, Y. 2015.** The I-TASSER Suite: protein structure and function prediction. *Nature Methods* **12**, 7-8.

**Yang, Q., Meng, D., Gu, Z., Li, W., Chen, Q., Li, Y., Yuan, H., Yu, J., Liu, C., and Li, T. 2018.** Apple S-RNase interacts with an actin-binding protein, MdMVG, to reduce pollen tube growth by inhibiting its actin-severing activity at the early stage of self-pollination induction. *Plant Journal* **95**, 41-56.

**Zhang, Y., Vuković, L., Rudack, T., Han, W., and Schulten, K. 2016.** Recognition of poly-ubiquitins by the proteasome through protein refolding guided by electrostatic and hydrophobic interactions. *Journal of Physical Chemistry* **120**, 8137-8146.

**Zhang, Y., Zhao, Z., and Xue, Y. 2009.** Roles of proteolysis in plant self-incompatibility. *Annual Review of Plant Biology* **60**, 21-42.

**Zhao, L., Huang, J., Zhao, Z., Li, Q., Sims, T.L., and Xue, Y. 2010.** The Skp1-like protein SSK1 is required for cross-pollen compatibility in S-RNase-based self-incompatibility. *Plant Journal* **62**, 52-63.

**Supporting Information**

Additional Supporting Information may be found online in the Supporting Information section at the end of the article.

**Fig. S1.** Identification of six ubiquitinated residues of *Petunia hybrida* $S_3$-RNase by LC-MS/MS analysis of cross-pollinated pistils.

**Fig. S2.** Two ubiquitinated residues of *Petunia hybrida* $S_3$-RNase identified by LC-MS/MS analysis of self-pollinated and unpollinated pistils.

**Fig. S3.** Locations of six ubiquitinated residues of *Petunia hybrida* $S_3$-RNase in Solanaceous S-RNases.

**Fig. S4.** *Petunia hybrida* $S_3$-RNase with the mutated region (R) I displays largely unaltered biochemical and physical properties.

**Fig. S5.** Physical interactions between *Petunia hybrida* $S_3$R/Mutant (M) and Ph$S_3$SLF1.

**Fig. S6.** Predicted three dimensional (3D) structures and surface electrostatic potentials of *Petunia hybrida* $S_3$-RNases with mutated ubiquitinated residues.

**Fig. S7.** *Petunia hybrida* $S_3R$ and $S_3R$ (*Mutant*) (*M*) transgenes identification by PCR analysis.

**Fig. S8.** Identification of *FLAG*-tagged *Petunia hybrida* $S_3R$ and $S_3R$ (*Mutant*) (*M*) transgenes by PCR analysis.

**Fig. S9.** Detection of *FLAG*-tagged *Petunia hybrida* $S_3R$ and $S_3R$ (*Mutant*) (*M*) transgenes expression by immunoblots.

**Fig. S10.** *Petunia hybrida* $S_3$-RNase with the mutated region (R) I slightly reduces cross seed sets.

**Fig. S11.** Decreased ubiquitination amount of mutant (M) I, II and III mediated by $SCF^{S_{3L}SLF1}$ of *Petunia hybrida*.

**Fig. S12.** Ubiquitination of *Petunia hybrida* $S_3$R and its mutant forms by self- ($PhS_3S_3$) pollen-tube extracts (PTE).

**Fig. S13.** Reduced seed set per capsule from $T_0$ transgenic lines with mutated region (R) II of *Petunia hybrida* $S_3$-RNase.

**Fig. S14.** Reduced seed set per capsule from $T_0$ transgenic lines with mutated lysine or threonine within the six ubiquitinated residues of *Petunia hybrida* $S_3$-RNase.

**Fig. S15.** Mutant **(**M) III largely maintains the biochemical and physical properties of *Petunia hybrida* $S_3$-RNase.

**Fig. S16.** *Petunia hybrida* $S_3$-RNase with mutated region (R) III markedly reduces cross seed sets.

**Fig. S17.** Largely unaltered physicochemical properties of *Petunia hybrida* $S_3$-RNase with mutated region (R) I, II and III.

**Fig. S18.** Reduced seed set per capsule from $T_0$ transgenic lines with mutated region (R) I/II/III of *Petunia hybrida* $S_3$-RNase.

**Table S1.** List of primer sequences.

**Table S2.** Names and accession numbers of S-RNases used in this study.

**Table S3.** Seed sets of *$S_3S_{3L}$*/*$S_3R$* and *$S_3S_{3L}$*/*$S_3R$* (*Mutant*) (*M*) $T_0$ transgenic plants of *Petunia hybrida*.

**Table S4.** Seed sets of *$S_3S_{3L}$*/*$S_3R$-FLAG* and *$S_3S_{3L}$*/*$S_3R$* (*Mutant*) (*M*)-*FLAG* $T_0$ transgenic plants of *Petunia hybrida*.

**Figure legends**

**Fig. 1. Six amino acid residues of *Petunia hybrida* $S_3$-RNase are ubiquitinated by K48-linked polyubiquitin chains through $SCF^{PhS_{3L}SLF1}$.** **(a)** Immunoblot detection of *in vitro* ubiquitinated products of $PhS_3$-RNase by $PhS_{3L}$SLF1. The pollen genotypes and the transgene are indicated on top and $PhS_3S_{3L}$ used as a negative control. Brackets indicate polyubiquitinated $PhS_3$-RNases. Open and filled arrowheads indicate ubiquitin and unubiquitinated $PhS_3$-RNase monomers, respectively. Antibodies used are indicated in the bottom as ubiquitin (Ub), $PhS_3$-RNase, Ub-K48 and Ub-K63, respectively. K: lysine. FLAG: a protein tag. **(b)** Ubiquitination sites of $PhS_3$-RNase identified by LC-MS/MS. Ub: the amino acid residue on its right within the peptide sequence of $PhS_3$-RNase is ubiquitinated. The b- and y-type product ions are indicated. **(c)** The secondary structural features of $PhS_3$-RNase with the locations of the six ubiquitination sites. C1-C5, five conserved regions; Hva and Hvb, hypervariable region a and b. K, C and T: lysine, cysteine and threonine, respectively. **(d)** Spatial locations of the six ubiquitination sites on the three dimensional (3D) structure of $PhS_3$-RNase. The dark blue region indicates the Hv regions of $PhS_3$-RNase, the green the residues identified by LC-MS/MS in unpollinated, self-pollinated and cross-pollinated pistils, and the cyan the residues identified specifically in cross-pollinated pistils. I, II and III: three regions containing the ubiquitination sites shown in the predicted 3D structure of $PhS_3$-RNase.

**Fig. 2**. ***Petunia hybrida*** **$S_3$-RNase with mutated region (R) II significantly inhibits cross seed sets. (a)** RNase activity detection of His-$S_3$R and mutant (M) II expressed by *pCold-TF* vectors. The relative fluorescence unit (RFU) indicating RNase activity during a time-course experiment is shown as mean ± S.D. (n = 3). II: the ubiquitinated region II of $PhS_3$-RNase. **(b)** Immunoblot detection of FLAG-tagged MII in subcellular fractions of *in vitro* germinated pollen tubes. EC1, EC2 and WTEC indicate entire cell homogenates of the pistils from the transgenic plants containing *MII-FLAG*, the pollen tubes of $PhS_VS_V$ treated with EC1 and the pistils from wild-type $PhS_3S_{3L}$. WTEC was a negative control. S1 and P1, S12 and P12, S160 and P160 indicate supernatant and pellet fractions obtained by centrifugation of EC2 at 1,000 g, 12,000 g and 160,000 g, respectively. cFBP and Sar1 are respective marker antibodies of cytosol and endoplasmic reticulum (ER). **(c)** Physical interactions between $PhS_{3L}$SLF1 and MII detected by pull-down assay. Input and pull-down: bait protein SUMO-His-$PhS_{3L}$SLF1 and prey proteins detected by immunoblots, respectively. MBP and SUMO-His are protein tags. Asterisks indicate bands of target proteins. **(d)** Split firefly luciferase complementation (SFLC) assay. The numbers on the left side of the color signal bars represent the values of the fluorescent signal. The injection positions of each component on tobacco leaves are indicated in the contour diagram of leaf margin. nLUC and cLUC indicate transiently expressed N-terminal and C-terminal regions of luciferase. **(e)** Bimolecular fluorescence complementation (BiFC) assay. NE and CE: transiently expressed N-terminal and C-terminal regions of YFP by *pSPYNE* and *pSPYCE* vectors. YFP, BF and Merge represent the YFP fluorescence, bright field and their merged field, respectively. Bars: 20 μm. **(f)** Transcripts of the transgene and native *$PhS_3$-RNase* detected by qRT-PCR. The $T_0$ transgenic lines are indicated below the horizontal axes. $S_3S_{3L}$ is a wild type. Data are shown as mean ± S.D. (n = 3). **(g)** Quantitative analyses of $S_3$R- and MII-FLAG proteins. The $T_0$ transgenic lines are indicated below the horizontal axes. Data are shown as mean ± S.D. (n = 3). A student's *t*-test was used to generate the *p* values. ns (not significant), $p > 0.05$. **(h)** Statistical analyses of seed sets per capsule from $T_0$ transgenic plants pollinated with cross pollen of $PhS_VS_V$. Data are shown as mean ± S.D. ($n \geq 9$). A student's *t*-test was used to generate the *p* values. **, $p < 0.01$. **(i)** Cell-free degradation of recombinant SUMO-His-MII by pollen-tube extracts (PTE) of $PhS_VS_V$ or

*$PhS_3S_3$*. Left, immunoblots of the reaction products incubated with or without MG132 (Mock). Start, time point zero in each degradation assay. cFBP antibody was used to detect non-degraded loading control. Right, quantitative analyses of the degradation rates. Data are shown as mean ± S.D. (n = 3). The remaining amount at 10 min is indicated. (**j**) Time-course analyses of $PhS_3$R- and MII-FLAG levels in the cross- (*$PhS_VS_V$*) or self- (*$PhS_3S_3$*) pollen tubes (PT) incubated with or without MG132 (Mock). *$PhS_VS_V$* and *$PhS_3S_3$* PT were challenged with style extracts of *$PhS_3S_{3L}$*/*$PhS_3$R-* or /*MII-FLAG* for 5 hours to mimic cross- and self-pollination, respectively. Top, immunoblots of $PhS_3$R- or MII-FLAG in the PT using FLAG antibody. cFBP was detected as a loading control. The numbers at the bottom indicate the transgenic line numbers corresponding to those in **h**. Bottom, quantitative analyses of the immunoblots. Data are shown as mean ± S.D. (n = 3). A student's *t*-test was used to generate the *p* values. **, $p < 0.01$.

**Fig. 3. K154 and K217 of the region (R) II of *Petunia hybrida* $S_3$-RNase serve as two major ubiquitination sites for its degradation in cross-pollen tubes. (a)** RNase activity detection of His-mutant (M) K and MT expressed by *pCold-TF* vectors. RFU: relative fluorescence unit. K and T: lysine and threonine within six ubiquitinated residues of $PhS_3$-RNase. Data represent mean ± S.D. (n = 3). **(b)** Immunoblot detection of FLAG-tagged MK and MT in subcellular fractions of *in vitro* germinated pollen tubes. EC1, EC2 and WTEC: entire cell homogenates of the pistils from the transgenic plants containing *MK*- or *MT-FLAG*, the pollen tubes of $PhS_VS_V$ treated with EC1 and the pistils from wild-type $PhS_3S_{3L}$. S1, P1, S12, P12, S160 and P160: supernatant and pellet fractions obtained by centrifugation of EC2 at 1,000 g, 12,000 g and 160,000 g, respectively. cFBP and Sar1: respective marker antibodies of cytosol and endoplasmic reticulum (ER). **(c)** Physical interactions between $PhS_{3L}$SLF1 and MK and MT detected by pull-down assays. MBP and SUMO-His: protein tags. **(d)** SFLC assays. nLUC and cLUC: transiently expressed N-terminal and C-terminal regions of luciferase. **(e)** BiFC assays. NE and CE: transiently expressed N-terminal and C-terminal regions of YFP. YFP, BF and Merge: the YFP fluorescence, bright field and their merged field, respectively. Bars: 20 μm. **(f)** Transcripts of transgene and native *$PhS_3$-RNase* detected by qRT-PCR. Data are shown as mean ± S.D. (n = 3). Student's *t*-test: **, $p < 0.01$. **(g)** Quantitative analyses of $S_3$R-, MK- and MT-FLAG proteins. Data are shown as mean ± S.D. (n = 3). Student's *t*-test: ns (not significant), $p > 0.05$; **, $p < 0.01$. **(h)** Statistical analyses of seed sets per capsule from $T_0$ transgenic plants pollinated with cross pollen of $PhS_VS_V$. Data are shown as mean ± S.D. (n = 10). Student's *t*-test: ns (not significant), $p > 0.05$; **, $p < 0.01$. **(i)** Immunoblots of recombinant SUMO-His-MK and -MT in the cell-free degradation products incubated by $PhS_VS_V$ pollen-tube extracts (PTE) with or without MG132 (Mock). Data are shown as mean ± S.D. (n = 3). **(j)** Immunoblot detection of *in vitro* ubiquitination products of His-$S_3$R, -MK and -MT by $SCF^{PhS_{3L}SLF1\text{-}FLAG}$ (E3) using anti-ubiquitin (Ub) and -His antibodies. The vertical lines illustrate the ubiquitinated substrates. Open and filled arrowheads indicate ubiquitin and unubiquitinated substrate monomers, respectively. Annotations of this figure are identical to those of Fig. 2.

**Fig. 4. *Petunia hybrida* $S_3$-RNase with mutated region (R) I, II and III regions significantly reduces cross seed sets. (a)** Transcripts of the transgene (*$PhS_3$-RNase or mutant* (*M*) *I*/*II*/*III*) and native *$PhS_3$-RNase* detected by qRT-PCR. Data are shown as mean ± S.D. (n = 3). Student's *t*-test: **, $p < 0.01$. I, II and III, three ubiquitination regions of $PhS_3$-RNase. FLAG, a protein tag. **(b)** Quantitative analyses of $S_3$R- and MI/II/III-FLAG proteins. Data are shown as mean ± S.D. (n = 3). Student's *t*-test: ns (not significant), $p > 0.05$. **(c)** Statistical analyses of seed sets per capsule from $T_0$ transgenic lines containing *MI*/*II*/*III* pollinated with cross pollen of $PhS_VS_V$. Data are shown as mean ± S.D. (n = 10). Student's *t*-test: ns (not significant), $p > 0.05$; **, $p < 0.01$. **(d)** Immunoblots of recombinant SUMO-His-MI/II/III in the cell-free degradation products incubated in the pollen-tube extracts (PTE) of $PhS_VS_V$ or $PhS_3S_3$ with or without MG132 (Mock). Data represent mean ± S.D. (n = 3). **(e)** Time-course analyses of MI/II/III-FLAG amounts in the cross- ($PhS_VS_V$) or self- ($PhS_3S_3$) pollen tubes (PT) incubated with or without MG132. Data are shown as mean ± S.D. (n = 3). Student's *t*-test: **, $p < 0.01$. **(f)** Immunoblot detections of *in vitro* ubiquitinated recombinant His-tagged $S_3$R and MI/II/III. Annotations of this figure are identical to those of Fig. 2 and 3.

**Fig. 5. Proposed model for a stepwise ubiquitination and degradation mechanism of *Petunia hybrida* S-RNases.** Self- and non-self S-RNases (SR and NR) and their region (R) I ubiquitinated forms can enter the cytoplasm through the pollen tube membrane. The R I ubiquitinated S-RNases could be degraded by the 26S proteasome, whereas their unubiquitinated forms are identified by SLFs. SR and its cognate SLF repel each other and results in an inability of $SCF^{SLF}$ to ubiquitinate SR. In contrast, NR is attracted by non-self SLF for R II ubiquitination by $SCF^{SLF}$ and its subsequent degradation by the 26S proteasome. Subsequently, internal R III could be further exposed for ubiquitination, leading to degradation of NR by the 26S proteasome or other unknown pathways. In addition, S-RNase compartmentalization could occur in the vacuole and contribute to its sequestration. I, II, and III: three ubiquitination regions in S-RNases.

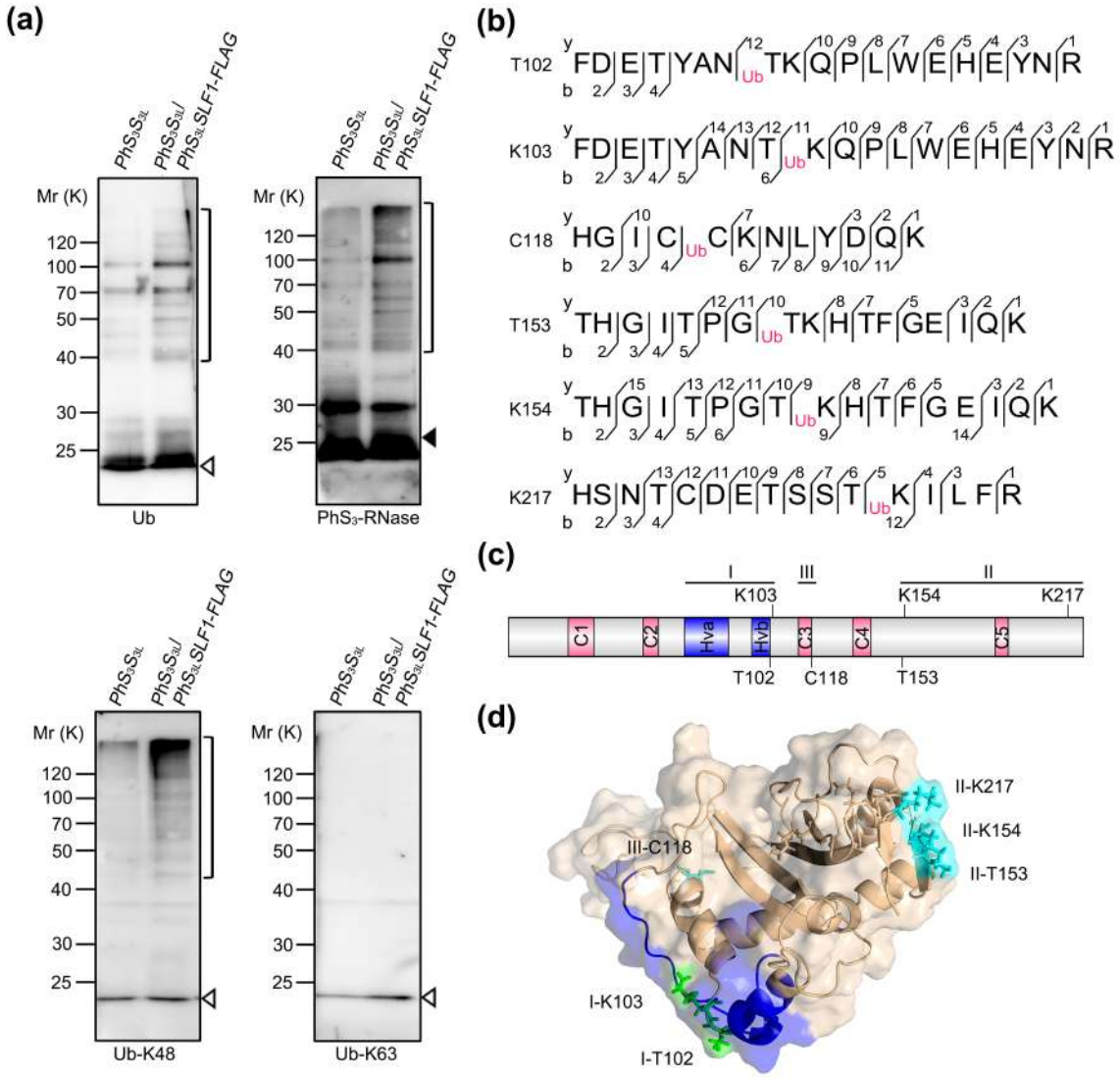


nph_17438_f1.tif

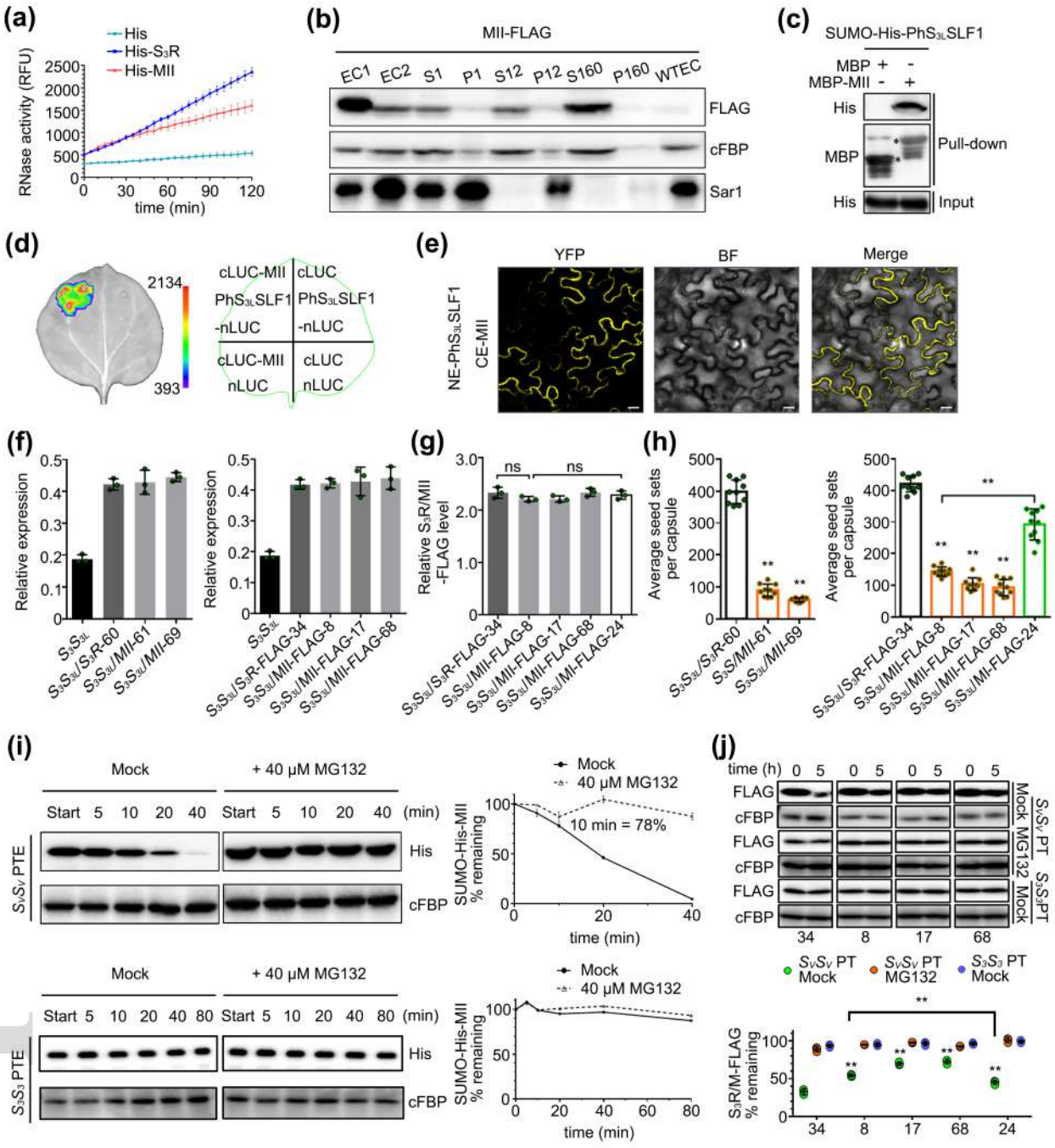


nph_17438_f2.tif

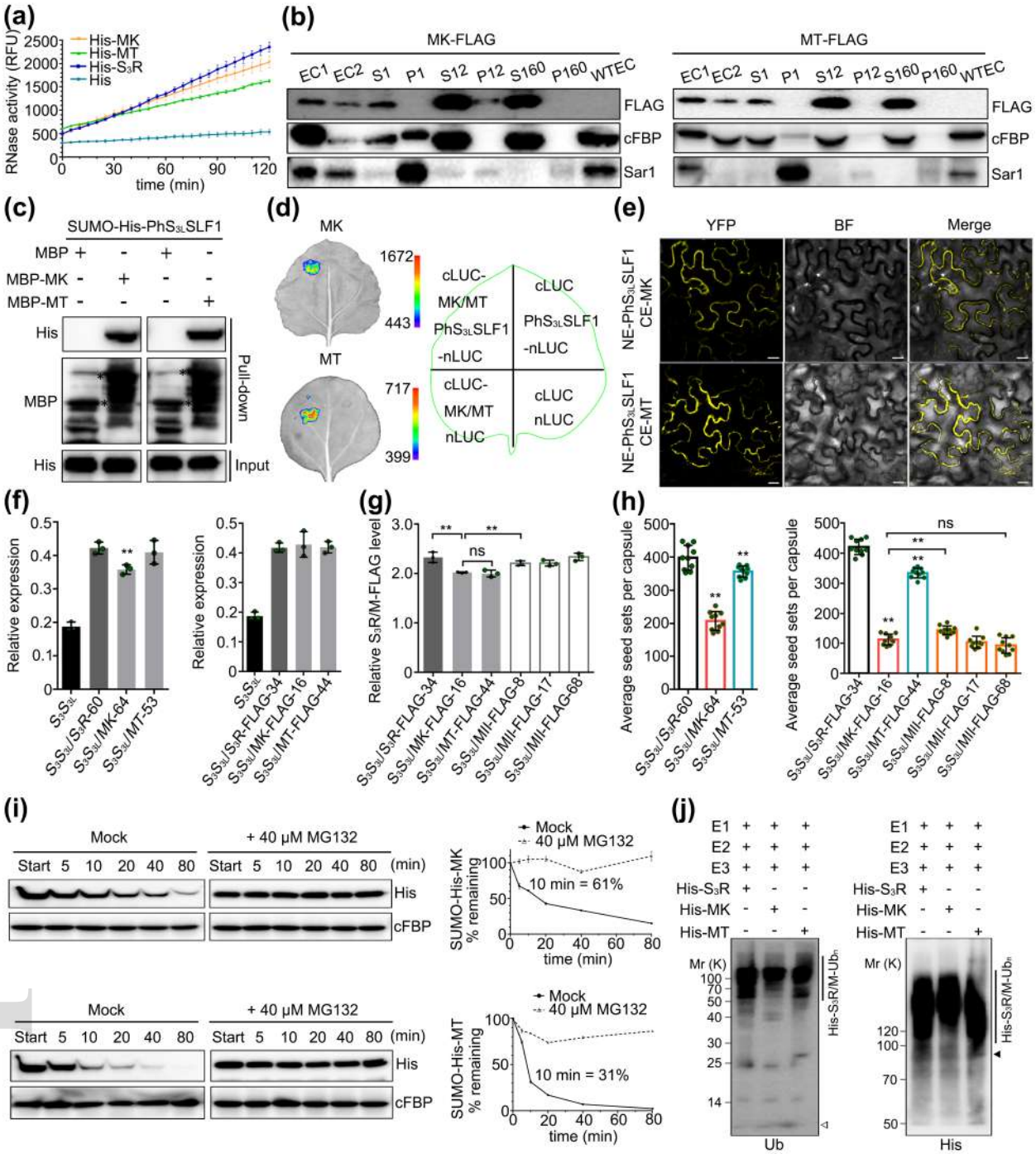


nph_17438_f3.tif

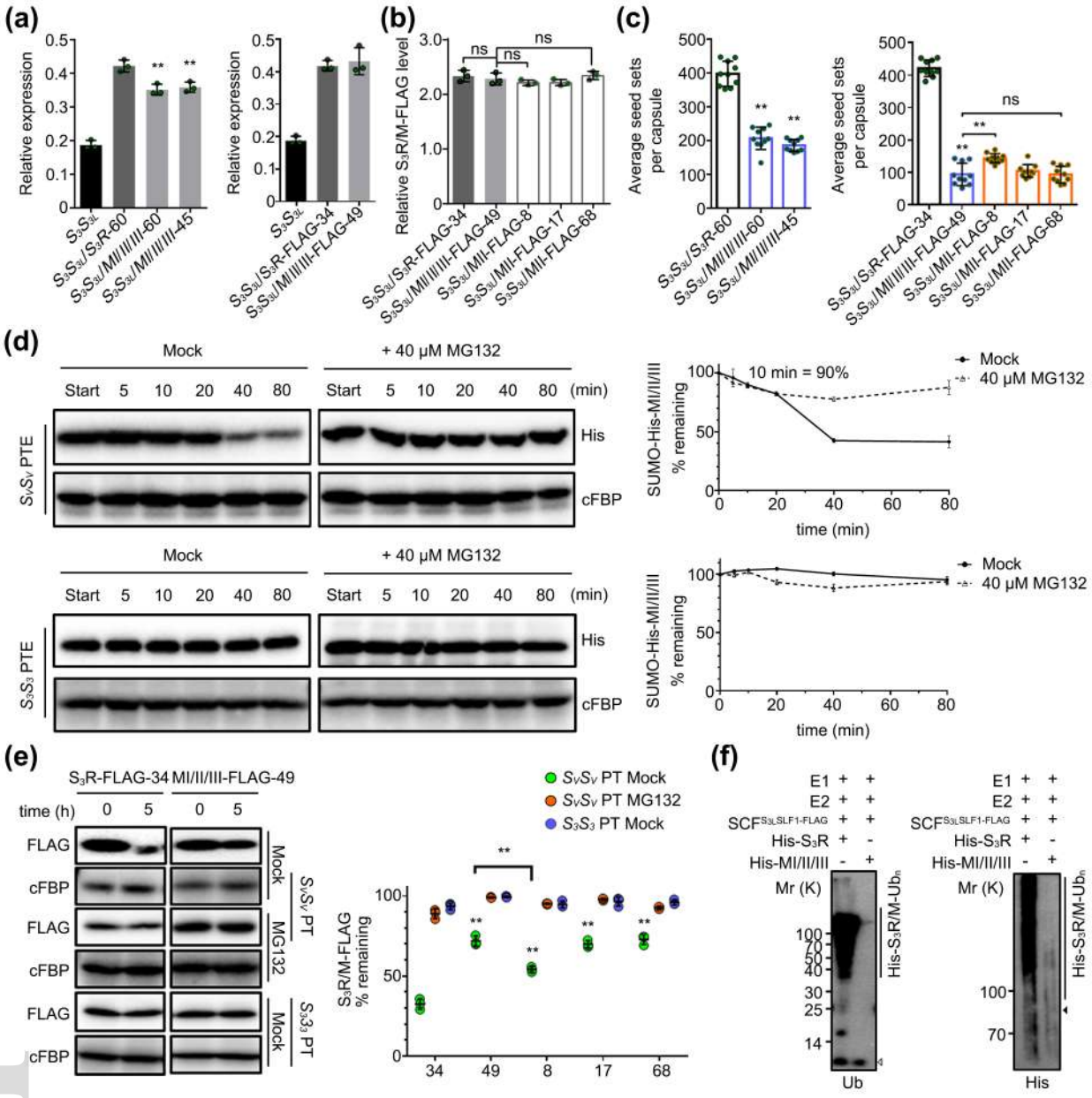


nph_17438_f4.tif

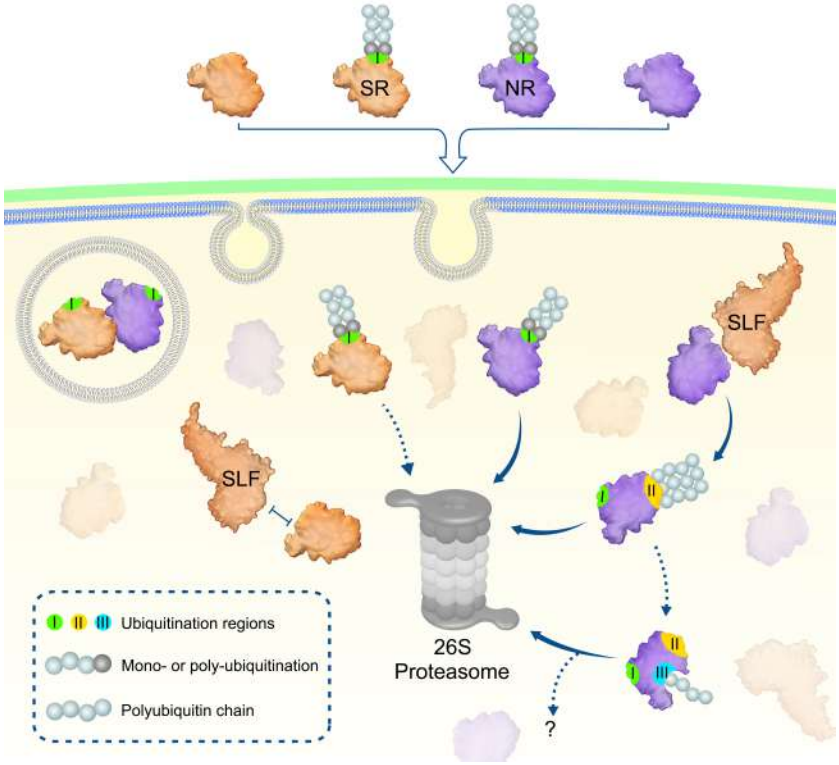


nph_17438_f5.tif